Sensitivity of Vegetation in India to Climatic Factors at Multiple Timescales

A Thesis submitted to

Indian Institute of Science Education and Research, Pune in partial fulfilment of the requirements of the BS-MS Dual Degree Programme

by

Kunjal Parnami

Date: October, 2023

Under the guidance of

Supervisor: Prof. Sumanta Bagchi,

Centre for Ecological Sciences, Indian Institute of Science

From January 2023 to October 2023

INDIAN INSTITUTE OF SCIENCE EDUCATION AND RESEARCH, PUNE

DR. HOMI BHABHA ROAD, PASHAN, PUNE- 411008, INDIA.

Certificate

This is to certify that this dissertation entitled *'Sensitivity of Vegetation in India to Climatic Factors at Multiple Timescales'* towards partial fulfilment of the BS-MS dual degree programme at the Indian Institute of Science Education and Research, Pune, represents study/work carried out by Kunjal Parnami at the Indian Institute of Science under the supervision of Sumanta Bagchi, Associate Professor, Centre for Ecological Sciences, during the academic year 2022-2023.

Sumanta Bagchi

Sumanta Bagchi

Project Supervisor

Associate Professor

CES, Indian Institute of Science

Date: 31 December 2023

Declaration

I hereby declare that the matter embodied in the report entitled *'Remote-Sensed Sensitivity of Indian Vegetation to Climatic Factors, at Multiple Timescales'* is the result of the work carried out by me at the Centre for Ecological Sciences, Indian Institute of Science, under the supervision of Prof. Sumanta Bagchi, and the same has not been submitted elsewhere for any other degree.

Kunjal Parnami

BS-MS Student, IISER Pune

Registration no. 20181050

Date: 31 December 2023

Acknowledgments

I thank my supervisor, Sumanta Bagchi, for giving me this opportunity, and facilitating and guiding me through this past year. I am grateful for the freedom to explore and to choose a topic I found interesting. I am also grateful to my labmates at the Ecosystems Lab, who made it an engaging and welcoming place to work. I am especially indebted to Dilip Naidu for his extensive guidance with my project. I also appreciate the broader CES community for making the department a lively and friendly environment.

I am so thankful for the support of all my friends, whose constant encouragement has kept me motivated through these challenging months. I am grateful for my family and their unconditional love. I am indebted to IISER Pune for giving me an environment that has shaped me into who I am today. I have met so many amazing people and learnt so much, and I truly feel these have been the happiest and most exciting years of my life so far.

Finally, I am grateful for the support of the KVPY fellowship (funded by DST, GoI) during my degree.

Abstract

In order to predict and model the responses of vegetation to future climate change, it is essential to understand vegetation responses to climate. In this study I used kNDVI, temperature, vapour pressure deficit (VPD), and rainfall data to calculate the sensitivity of vegetation to climate in the Indian mainland. Here, vegetation sensitivity to a climate variable refers to the response of vegetation to a unit change in that variable. Sensitivity is estimated as the regression coefficients from a fitted multiple linear regression.

I used STL decomposition to separate kNDVI time series into 3 timescales—trend, seasonal and remainder. The seasonal component is dominant and explains 80% of variation in the original time series. The remainder component explains about 15%.

To examine sensitivity to climate at different timescales, each of the STL components (as well as the complete kNDVI time series) was regressed against standardised climate variables. The sensitivity data—for each climate variable and kNDVI component—was examined spatially, and also correlated against the other sensitivities to reveal any interesting relationships. The sensitivities of the seasonal-component and complete kNDVI models are strongly correlated. For all models/components, temperature-sensitivity is negatively correlated with both rain- and VPD-sensitivity, while rain-sensitivity is positively correlated with VPD-sensitivity.

The sensitivities of vegetation to climate variables were then split by vegetation type—there were no significant differences in mean sensitivity. All vegetation types in India seem to respond similarly to climate. To check for relations between sensitivity and long-term or background climate, the vegetation sensitivity data were correlated with mean climate data and squared climate data. No clear relationships were identified. More study is needed to fully characterise vegetation dynamics in India.

Contributions

Contributor name	Contributor role
Kunjal Parnami, Dilip Naidu, Sumanta Bagchi	Conceptualization of Ideas
Kunjal Parnami, Dilip Naidu	Methodology
Kunjal Parnami	Software
Kunjal Parnami	Validation
Kunjal Parnami	Formal analysis
Kunjal Parnami	Investigation
Sumanta Bagchi	Resources
Dilip Naidu, Kunjal Parnami	Data Curation
Kunjal Parnami	Writing - original draft preparation
Kunjal Parnami, Sumanta Bagchi	Writing - review and editing
Kunjal Parnami	Visualization
Sumanta Bagchi	Supervision
Sumanta Bagchi	Project administration
Sumanta Bagchi	Funding acquisition

Table of Contents

List of Figures

List of Tables

Introduction

Vegetation is an essential component of the biosphere, and is also a key player in the carbon cycle. Terrestrial vegetation modulates the carbon cycle by absorbing carbon dioxide at the biosphere-atmosphere interface, storing it in vegetative matter (Farquhar, 1997), influencing the size of carbon reservoirs in the soil and living vegetation (Sedjo and Sohngen, 2012; Terrer *et al.*, 2021), affecting local climate (Green *et al.*, 2017; Alkama *et al.*, 2022), and more. Climate change and other anthropogenic activities—like the expansion of agriculture, nitrogen pollution, land-use change, etc.—are having significant impacts on terrestrial vegetation (Canadell *et al.*, 2021), which in turn may alter its feedback on the climate. It is important to understand the exact ways in which terrestrial vegetation will respond to these changes. The response of vegetation to changing climatic conditions needs to be well-understood in order to accurately predict, mitigate or adapt to it.

Such changes are likely to be especially pronounced in India, which is projected to experience serious impacts due to climate change in the coming decades (ed.Intergovernmental Panel on Climate Change (IPCC), 2023). The focal region of this study is the Indian mainland. India is climatically under the regime of the south-west monsoon, which delivers over 75% of India's total rain (Parida *et al.*, 2020). The north-east winter monsoon also delivers rain to parts of the country. The climate can be represented by four seasons—winter (January to February), pre-monsoon (March to May), monsoon (June to September), and post-monsoon (October to December) (India Meteorological Department. (last), 2017). Vegetation growth is determined by this distinct pattern of monsoon rainfall. The pattern of the monsoon rains has been changing for the last few decades (Guhathakurta and Rajeevan, 2008) and the mean temperature has been slowly rising (Gulev *et al.*, 2021). India is home to a diversity of biomes and vegetation types. Apart from India's diverse natural vegetation, much of Indian agriculture is also primarily dependent on a favourable climate and rain for sufficient growth and yield (ed.Intergovernmental Panel on Climate Change (IPCC), 2023). Understanding the responses of both natural and agricultural vegetation to climate is thus important to predicting and preparing for the future.

In order to understand the responses of Indian vegetation to climate, I have undertaken this study to examine the response strength of vegetation to temperature, precipitation and VPD, using satellite remote-sensing data. I used kNDVI (kernel- Normalised Difference Vegetation Index) as a proxy for vegetation biomass (Camps-Valls *et al.*, 2021). NDVI is a metric that has strong correlations with vegetation cover, vegetation greenness, biomass, or Leaf Area Index. It is widely used as it is reliable, performs well, and NDVI datasets cover longer time periods than other vegetation indices (Pettorelli *et al.*, 2005). The GIMMS NDVI data series is one of the longest series of data, from 1982 to 2013. Nonetheless it has problems, such as saturation at high levels of vegetation coverage, in regions like rainforests. The simplified kernel NDVI improves utilisation of information from the near-infrared (NIR) and red (R) bands (from which NDVI is calculated), reduces saturation effects, and propagates lower uncertainty (Camps-Valls *et al.*, 2021).

Many studies have used satellite NDVI to explore the strength of terrestrial vegetation's responses to climate, on a regional (Guhathakurta and Rajeevan, 2008; Deng *et al.*, 2013; Parida *et al.*, 2020; Diao *et al.*, 2021; P. and Paul, 2021) and global scale (Wu *et al.*, 2015; Seddon *et al.*, 2016; Liu *et al.*, 2018; Kusch *et al.*, 2022). Such studies focus on any number of a wide variety of climate or environmental variables as drivers of NDVI responses—such as temperature, precipitation, incoming radiation, soil moisture, etc. Temperature and precipitation are the most commonly considered, sometimes with lags with respect to vegetation (Wu *et al.*, 2015; Seddon *et al.*, 2016; Ding *et al.*, 2020).

One way to understand vegetation responses to mean climate is to consider the response of vegetation to a unit change in a climatic variable. The sensitivity of vegetation to a climate variable is the change in the vegetation index due to a unit change in that climate variable. It can be conceptualised as the slope of the line fitted to vegetation versus climate. For cases with multiple climate variables as drivers, the sensitivity to any one climatic variable would be the corresponding regression coefficient from the fitted multivariate linear regression—that is, sensitivity is the change in vegetation index upon a unit change in one climate variable, given that all other variables are held constant.

Such a sensitivity metric was used by Liu *et al.* (2018), in comparing the sensitivity of vegetation to precipitation, with and without memory effects. Bao *et al.* (2021) used the fractional change in NDVI, divided by fractional change in the climate variable, as a measure of vegetation sensitivity to climate change. They found that the sensitivity was non-linear and varied with climatic zones (i.e., the mean climate of the area)—NDVI was more sensitive to temperature increase in colder seasons than that in warmer seasons. Abel *et al.* (2021) also used the slope of vegetation against rainfall to characterise the sensitivity of vegetation to rainfall in drylands. Zhang *et al.* (2022) estimated sensitivity of dryland vegetation to precipitation as the regression coefficient for precipitation from a multivariate linear regression.

Examining how vegetation sensitivity changes, and how it is affected by factors like climate, environmental variables like fire, human pressure, etc can help us uncover the mechanisms behind vegetation dynamics under different conditions. While some papers use 'sensitivity' to refer to the correlation coefficient between vegetation and the climatic variable(s) that drive it (Wang *et al.*, 2003; Piao *et al.*, 2006; Wang and Fan, 2021; Li *et al.*, 2022), I have not used such a definition. This is because I am trying to understand the magnitude of vegetation's response to a unit change in a climate variable. 'Sensitivity', in the sense that I use it, also has no connection with the concepts of ecosystem stability or resilience.

One important aspect of vegetation response/sensitivity to change in climate is that of time-scales. Responses of vegetation to climate may differ between the interannual, seasonal and intra-annual or monthly time-scales. Multiple studies looked at the relations between climate and NDVI variation at the level of different timescales, and found varying results across scales (He *et al.*, 2012; Nie *et al.*, 2012; Wang *et al.*, 2014). In order to examine the responses of vegetation at different timescales, I used the STL method (Seasonal-Trend decomposition using Loess) to split the vegetation time-series into 3 components—the long-term trend, the fixed-period seasonal, and the short-term remainder timescale components. STL is an additive time-series decomposition method that splits a discrete time series into the aforementioned 3 components using Loess polynomial fitting to smooth the seasonal and trend components (Cleveland *et al.*, 1990). The response of the different kNDVI time-scale components to climate is an important question.

Another aspect of the vegetation response to climate is the variations in vegetation sensitivity/responses with varying background (or long-term mean) climates. For example, Bao *et al.* (2021) found that vegetation is more sensitive to rainfall in drier regions, and more sensitive to temperature in colder areas.

The objectives of this study were to examine and answer, for the Indian mainland, the following questions:

a) How do the seasonal, trend and remainder timescales—different components split by STL decomposition—contribute to the original kNDVI time series?
b) How do these three components, indicating variations in vegetation on three different timescales, respond to climate variables?
c) How do the sensitivities (of the overall kNDVI time series, and its components at different timescales) vary spatially across India, and between different vegetation types?
d) What are the relationships between all these sensitivities?
e) How is sensitivity (of each of the components to different climate variables) in turn related to background climate?

Materials and Methods

Study area:

The chosen study area is the Indian mainland. India spans a large area, ranging from latitudes 8°4' N to 37°6' N, and 68°7' E to 97°25' E longitude. It covers areas within both the tropics and subtropics, and encompasses a wide range of biomes, climatic zones, and land and soil types. The climate is largely dominated by the annual South-West monsoons (India Meteorological Department. (last), 2017). Seasonal (summer-winter) oscillations also play a significant role, especially in the northern regions that are farther away from the Equator.

According to Koppen-Geiger climate classifications, India experiences a tropical monsoon climate in the Western Ghats region, tropical wet/tropical dry climate in the eastern part of the peninsula and central India, hot desert climate in the far north-west (Thar desert), and hot semi-arid climate in the northwest, as well as in the eastern peninsular region like Maharashtra and Karnataka (Peel *et al.*, 2007). The Gangetic plains and North India experience a monsoon-influenced humid subtropical climate. The higher reaches of the Himalayas experience tundra-like climate conditions. Figure 1 illustrates the mean kNDVI and climatic conditions (rain, temperature, VPD) across India, calculated from monthly data over 3 decades.

Figure 2, using data from the USGS Global Land Cover Characteristics Data Base Version 2.0, shows that India is dominated by cropland or mixed cropland/natural vegetation land cover types. It further shows the distribution of natural vegetation, with the north-west desert regions having sparsely-vegetated or shrubland areas, the northern region and Gangetic plain dominated by dryland or irrigated cropland and pasture, and the northeastern regions and the Western Ghats covered by forests. Central-eastern India has extensive tracts of savanna and deciduous broadleaf forests interspersed with cropland, while the northern Himalayan regions are covered by a variety of land-cover types like shrubland, grassland, wooded tundra, and unvegetated land and ice.

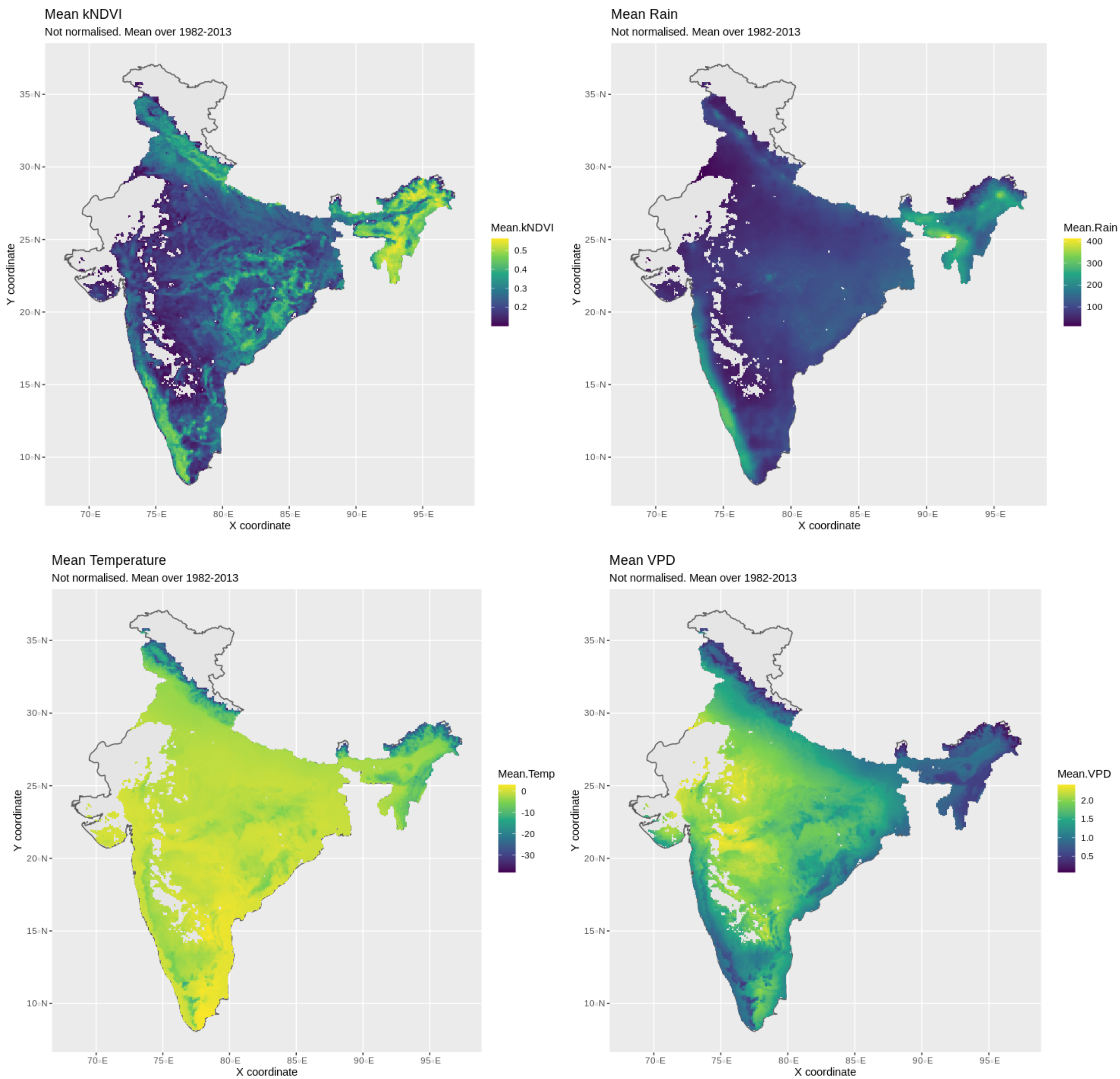

Figure 1: Maps showing the mean kNDVI and climate variables in the study area (not normalised, mean over all time-points from 1982 to 2013). From left to right: mean kNDVI, rain, temperature and VPD (vapour pressure deficit).

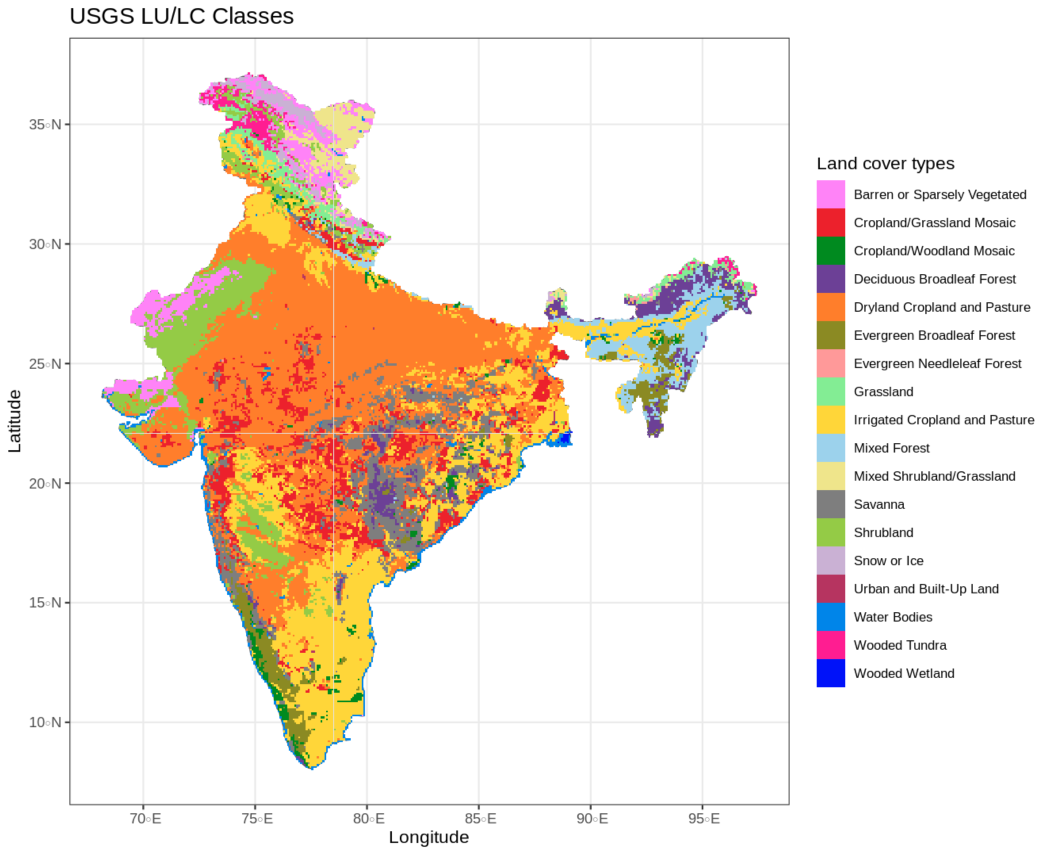

Figure 2: Map of India showing land use/ land cover classes from the Global Land Cover Characteristics Data Base, version 2.0 (classes are from the USGS (United States Geological Survey) Land Use/Land Cover System thematic map, and the map was constructed from AVHRR data over 1992-93).

Data:

kNDVI:

I used kNDVI (kernel Normalised Difference Vegetation Index) as a measure of the vegetation greenness. NDVI is a very widely used vegetation index, primarily due to its reliability and very long observational record—the GIMMS dataset is one of the longest, and spans almost 3 decades. It is effective at measuring greenness or chlorophyll content, and shows decent correlations with measures like leaf area index (LAI), or fractional vegetation cover (FVC) (Pettorelli *et al.*, 2005).

In order to account for its shortcomings (such as its saturation at high levels of vegetation), Camps-Valls *et al.*, 2021 developed a kernel NDVI that generalises the family of VIs based on differences and ratios of spectral bands. kNDVI can better cope with saturation effects, and propagates lower uncertainty than other indices. The simplified version, which I used in my analysis, is:

$$kNDVI = tanh(NDVI^2)$$

The NDVI data was obtained from the third generation GIMMS NDVI dataset (NDVI3g) derived from AVHRR (Advanced Very High Resolution Radiometer) sensors. This is the latest version of the GIMMS vegetation index data. It spans from 1982 to 2013, with a monthly temporal resolution. The data has been corrected for clouds, volcanic eruptions, and other errors by using data from multiple sensors, calibrating it, and using maximum-value compositing to give maximum monthly NDVI values (as errors generally lower the NDVI). The original data has a spatial resolution of 1/12 degree latitude, but was resampled to a resolution of 1/24 degree, which is that of the TerraClimate monthly data.

Temperature:

In this analysis I use data on monthly mean temperature, which was obtained by taking the average of the monthly maximum and minimum air temperature TerraClimate datasets. TerraClimate is a global dataset of monthly climate variables spanning from 1958 to 2019, with a spatial resolution of 1/24 degree latitude and longitude. I used a subset of the data, spanning from 1982 to 2013. TerraClimate data was developed using climatically-aided interpolation, and combines the high-spatial-resolution, climatological normals from the WorldClim dataset and coarser-spatial-resolution, time-varying data from CRU Ts4.0 and JRA55 (Abatzoglou *et al.*, 2018).

VPD:

Gridded Vapour Pressure Deficit data was obtained from TerraClimate, a global dataset of monthly climate variables spanning from 1958 to 2019. For this analysis, I use a subset of data for the time range of 1982 to 2013. The Terraclimate dataset has a spatial resolution of 1/24 degree latitude and longitude (which is about 4 km) (Abatzoglou *et al.*, 2018).

The vapour pressure deficit (VPD) data is derived from the primary climate variables (temperature and relative humidity, which is derived from the vapour pressure measure).

$$VPD = vp_{sat} \times \left(1 - \frac{relative\ humidity}{100}\right),$$

where vp_{sat} = saturation vapour pressure, which depends on temperature, and relative humidity can be calculated from the absolute vapour pressure data.

Potential Evapo-Transpiration (PET):

PET data was also taken from the TerraClimate dataset, for the time period 1982-2013. Like the other TerraClimate datasets, it had a monthly temporal resolution and 1/24 degree spatial resolution (Abatzoglou *et al.*, 2018). Potential EvapoTranspiration is defined as the amount of evaporation/transpiration that would occur if sufficient water were available. The TerraClimate PET data was estimated from primary TerraClimate variables (temperature, precipitation, vapour pressure) using the ASCE Penman-Monteith equation.

Rainfall:

Rainfall data was obtained from CHIRPS v2.0 (Climate Hazards Group InfraRed Precipitation with Station data), which is a gridded rainfall time series spanning from 50° North to 50° South, and all longitudes (Funk *et al.*, 2014). CHIRPS is produced by the Climate Hazards Center at UC Santa Barbara (in collaboration with the USCS EROS Center) by incorporating satellite imagery, climatology, and in-situ station data. It has a spatial resolution of 0.05 x 0.05 degrees. From this data, I extracted data for the coordinates corresponding to the TerraClimate monthly temperature dataset. The time series of CHIRPS spans from 1981 to the near-present. I used the CHIRPS monthly time-series, which measures total monthly rainfall in mm, from 1982 to 2013.

All the datasets were masked to only include points within India, and the values of all datasets were extracted for the same coordinates (the coordinates from the TerraClimate monthly temperature data).

Land Cover:

The Global Land Cover Characteristics Data Base version 2.0 is a 1-km resolution database, developed by the USGS (US Geological Survey), the EROS (Earth Resources Observation and

Science) Center, University of Nebraska-Lincoln (UNL) and the Joint Research Centre of the European Commission.

It is derived primarily from 1-km AVHRR (Advanced Very High Resolution Radiometer) NDVI data spanning a 12-month period from April 1992 to March 1993. The NDVI data was a 10-day composite product. While the NDVI composite is the core dataset used in characterising land-cover types, other data were also used—such as digital elevation maps, country-level or regional vegetation maps, land-cover maps, etc. This data was used to produce seasonal land cover regions using unsupervised classification and subsequent steps. These seasonal land cover regions were then translated into the Olson Global Ecosystem framework. The Olson Global Ecosystem land types were then translated into six other derived thematic maps.

Of these derived thematic maps, I am using the USGS (United States Geological Survey) Land Use/ Land Cover System thematic map. It was preferable as it separates irrigated and non-irrigated croplands, includes urban areas as a land cover class, and has a reasonable number of classes represented in India.

Methods

Normalisation, or standardisation:

The climate variable data were standardised and converted into z-scores.

$Z = \frac{x-\mu}{\sigma}$, where σ = standard deviation of the sample, and μ = mean of the sample.

This was done so that the model coefficients (or response strengths/sensitivities of kNDVI to the different climate variables) would be comparable. Specifically, the z-score normalisation for a climate variable was carried out using the mean and standard deviation of the variable across all pixels and time-points. The purpose of this choice was to maintain the relative values of the variable with respect to other pixels. This is in contrast to other papers (Ratzmann *et al.*, 2016; Liu *et al.*, 2018) that examined a similar metric of sensitivity or vegetation response to climate, but normalised each pixel individually.

Removing non-/sparsely-vegetated regions

Negative kNDVI values were omitted from the data. In order to exclude non-vegetated regions—such as bare soil, desert, man-made structures, water, etc.— or very sparsely-vegetated regions, pixels with mean kNDVI lower than 0.1 were excluded from consideration. This was done because any changes in the NDVI of such regions over time would likely be mechanistically unrelated to the climate, and show irrelevant patterns. The cut-off value of 0.1 was chosen on the basis of other studies using the same (Liu *et al.*, 2018).

Calculating sensitivity

For each pixel, a multivariable simple linear regression was fitted with kNDVI data as the dependent variable and normalised climate variables as the independent variables. The sensitivity of kNDVI at a given pixel, to a climate variable, is defined as the value of the regression coefficient for that particular variable.

Model choice/ Variable selection:

Starting with 4 climate variables (mean temperature, VPD, PET and rain), I carried out basic variable selection in order to choose the variables to include in the linear model, and eliminate problematic multicollinearity. From Figures 3 and 4, it is clear that PET is strongly positively correlated to VPD and temperature (correlation coefficient is about 0.9). The correlations between pairs of the other 3 variables (PET, rain, temperature) are smaller than 0.8, which is used as an approximate threshold for problematic multicollinearity (Kim, 2019). Thus I excluded PET from the model.

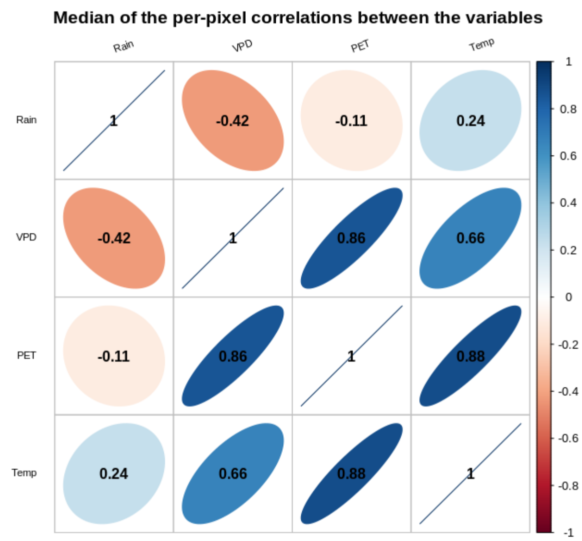

Figure 3: The figure shows the median correlations between the four climate variables for the study area. For each pixel, I calculated the pairwise linear correlation coefficients between the four climate variables (aka the correlation matrix). Then, I took the median, across pixels, of the correlation coefficients for each climate variable pair.

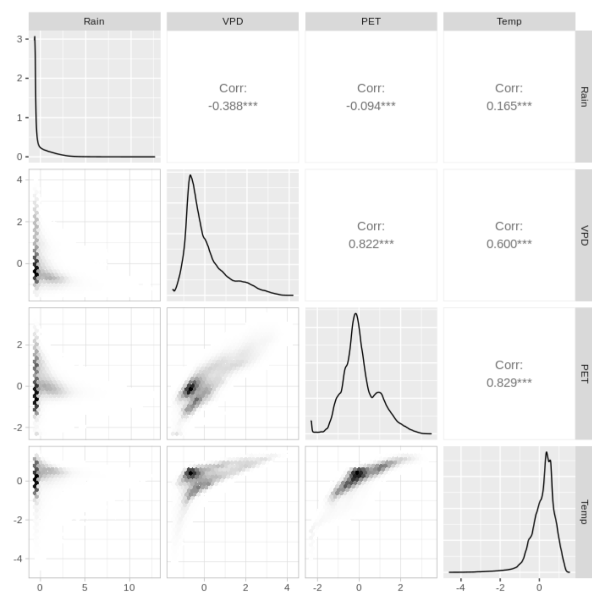

Figure 4: The upper triangular elements show the linear correlation coefficients between the climate variables (calculated from data combined across all pixels). Along the diagonal are the distributions of the four climate variable values (combined across all pixels and time-points). The lower triangular elements show the correlation plots of one climate variable against another (data combined across all pixels and time-points in the time-series).

Then, I checked the linear model, with the remaining 3 variables, for multicollinearity using Variance Inflation Factors (VIF) and Condition Indices (CIs) + Variance Decomposition Proportions (VDPs). The model was constructed with kNDVI and climate data combined across all pixels.

vpd_combined	temp_combined	rain_combined
2.533654	2.212286	1.665001

Table 1: Variance-inflation factors (VIF) for each of the variables in the model kndvi_combined ~ vpd_combined + temp_combined + rain_combined (the variables' data are combined across pixels).

The variance-inflation factor of an explanatory variable X_h is

$VIF = \frac{1}{1-R_h^2}$, where

$R_h =$ the coefficient of determination of a multi-variable linear model set up with X_h as the response variable and all other explanatory variables of the original model as the explanatory variables. That is, it is the amount of variation in one explanatory variable (X_h) that can be explained by all the other explanatory variables. If any of the VIFs is large (greater than 5 or 10), it indicates the presence of multicollinearity in the model (Kim, 2019).

From Table 1, we can see that none of the VIFs are large. This indicates the absence of significant multicollinearity in the model.

Serial no.	Condition Index	Variance Decomposition Proportions		
		vpd_combined	temp_combined	rain_combined
1	1.000	0.141	0.108	0.029
2	1.178	0.005	0.112	0.366
3	2.765	0.854	0.780	0.605

Table 2: Condition Indices and VDPs (variance decomposition proportions) for the linear model kndvi_combined ~ vpd_combined + temp_combined + rain_combined. The variables' data are combined across pixels.

Examining the condition indices is a regression model collinearity diagnostic procedure (Belsley, Kuh, and Welsch (1980)). There may be collinearity problems if the largest condition index (also called the condition number) is greater than 30. If a large condition index (greater than 10 to 30) is associated with two or more variables with large (> 50%) variance decomposition proportions, these variables may be causing collinearity problems (Kim, 2019). From Table 2, the Condition Number is only 2.765, and there are no large Condition Indices. These results suggest that there are no major collinearity problems in the model kNDVI ~ Rain + Temperature + VPD.

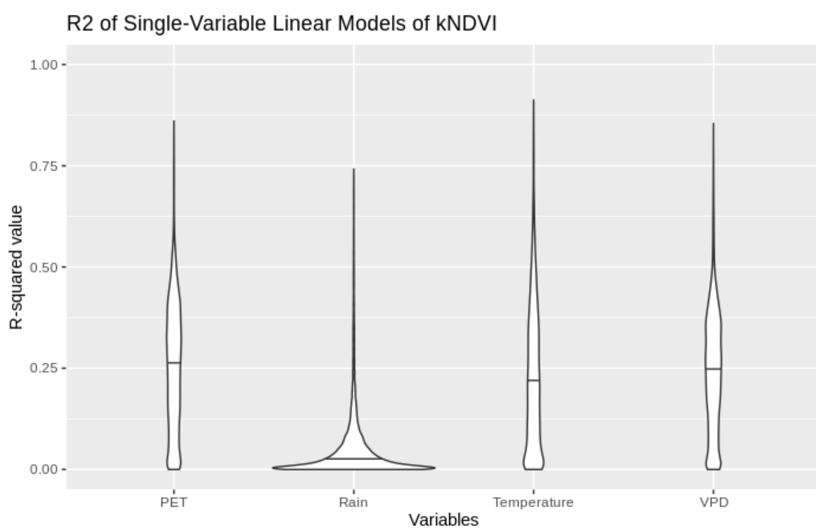

Figure 5: Plotting the distributions, across all pixels, of how well each variable individually explains the variability in kNDVI. Violin plots of the distributions of R-squared values of linear models fitting individual climate variables to the complete (not decomposed) kNDVI data

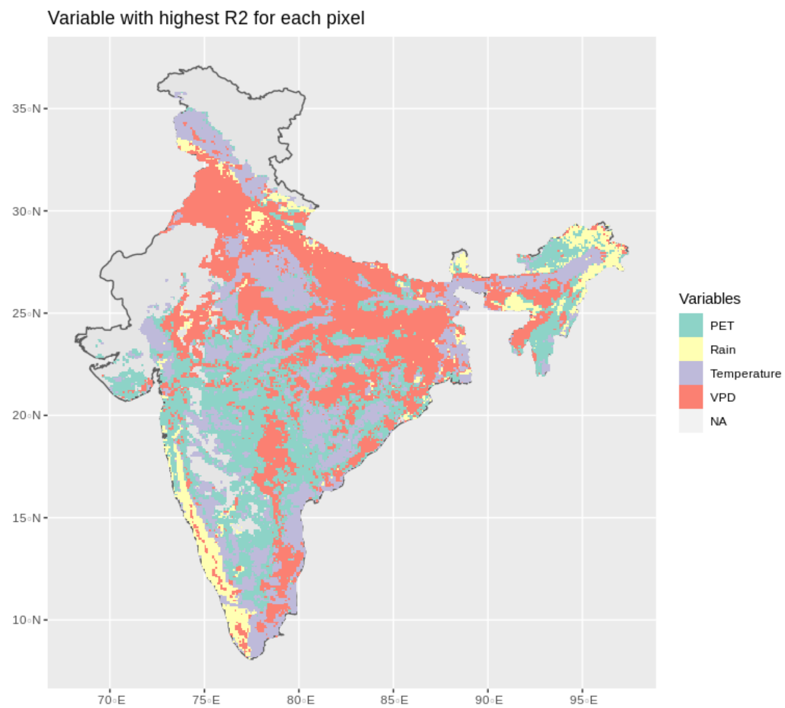

Figure 6: Map of the variable that best explains the complete kNDVI data at each pixel. That is, the variable whose corresponding single-variable model against kNDVI has the highest R-squared value, out of the four linear regression models of complete kNDVI against the normalised climate variables.

From Figures 5 and 6, it is clear that rain individually explains the least variation in complete kNDVI, as it is the primary or best explainer for very few pixels. VPD and temperature individually explain similar amounts of variation in kNDVI. PET is the best individual explanatory variable by a small margin, but it is still excluded due to its high correlation with the other variables.

STL:

Seasonal-Trend decomposition using Loess (STL) is an additive time-series decomposition method that splits a discrete time series into 3 components—a seasonal component of fixed period, a long-term trend component, and a remainder component (which covers the remaining short-term variation). I used STL to split the kNDVI time series of each pixel into its trend, seasonal and remainder timescale components. STL uses simple Loess polynomial fitting to smooth the seasonal and trend components, and the remainder time-series is found by subtracting the trend and seasonal components from the original time-series at every time point (Cleveland *et al.*, 1990).

The relative contribution or importance of each component to the complete kNDVI time-series can be found by linear regression of the complete time-series against the component time-series as the independent variable. The R-squared value of the regression indicates the contribution of the component to the complete time series, as it indicates the amount of variation in the original time-series that the component can explain. This R-squared value was plotted for all 3 components and all pixels.

Plotting the sensitivity and R-squared for the 4 models

Following the decomposition of the kNDVI series into 3 timescale components, the climate sensitivities of the 4 kNDVI time-series (the complete series and 3 components) were calculated for each pixel. The sensitivities and R-squared values of the 4 models were stored and plotted as maps, and the summary statistics of their distributions were plotted as boxplots or violin plots.

For each model, the variable with the largest absolute coefficient for each pixel was found and mapped. The variable with the largest absolute sensitivity value is the variable to which vegetation responds most strongly.

The relationships between the model coefficients were examined by calculating and plotting pairwise correlation matrices of the sensitivities to different climate variables, within each model. The same was done for the aggregated set of all sensitivities to the climate variables, across all four models.

Relation of sensitivity and mean climate variables

The sensitivities to each variable, for all models, were in turn correlated with the mean climate variables, or the background climate (averaged across all time points from 1982-2013). The correlation coefficients were plotted.

Analysis by land cover types:

In order to understand the variations in sensitivity between different vegetation types, the sensitivity data was subsetted by the USGS LU/LC land-cover classifications. The sensitivities of the subsets were then analysed.

Software:

All analyses were carried out in R (version 4.2.2 Patched (2022-11-10 r83330)) using RStudio 2022.02.2. The package ‘stlplus’ was used for carrying out STL decomposition on the kNDVI time-series. The packages ‘terra’, ‘stats’, ‘ggplot2’, ‘corrplot’, ‘GGally’, ‘zoo’, ‘xts’, ‘stlplus’, and ‘sf’ were also used.

Results and Discussion

Question 1: Importance of the STL Components to Complete Vegetation Dynamics

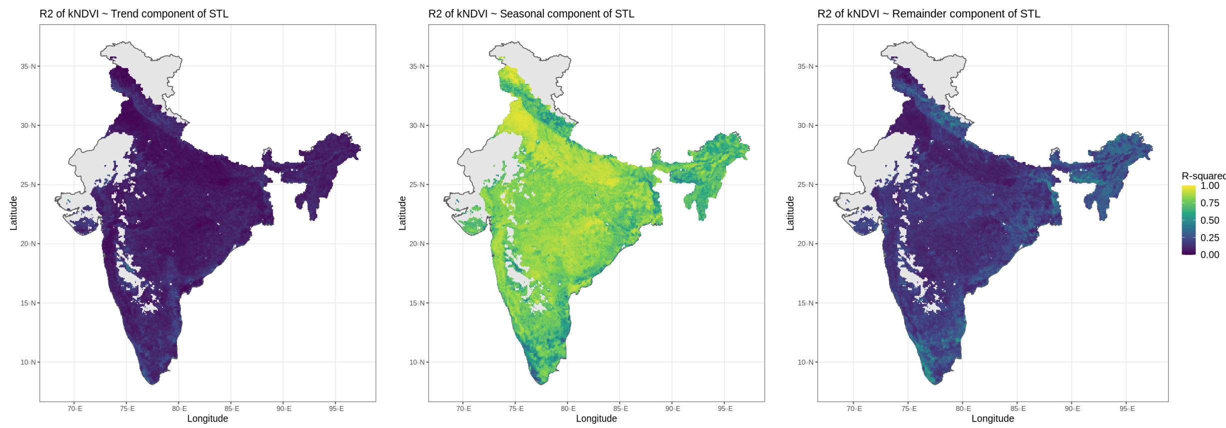

Figure 7: From left to right: maps of R-squared values of the correlations of kNDVI's Trend, Seasonal and Remainder STL components with the original (non-decomposed) kNDVI data. They show the contributions of the 3 components of kNDVI STL decomposition to the overall kNDVI time series.

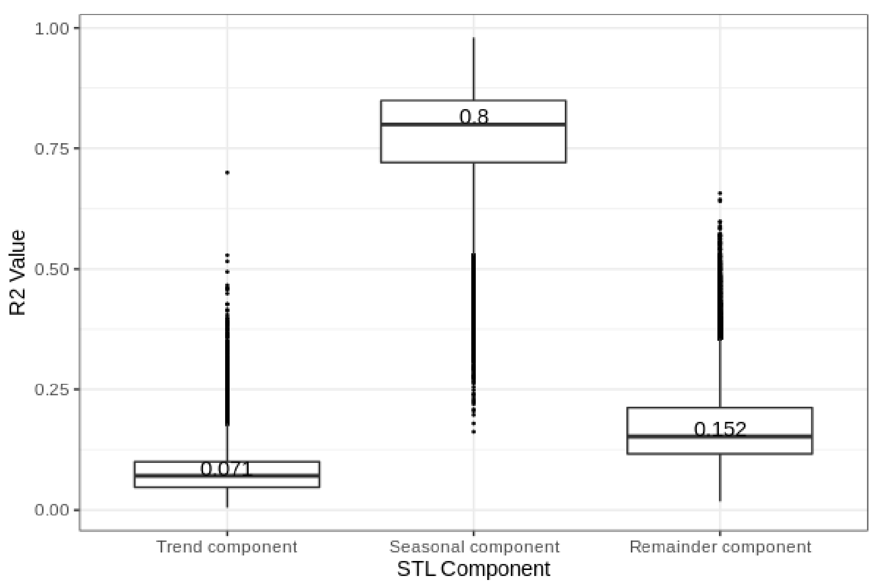

Figure 8: Boxplots of R-squared distributions for linear models of trend-, seasonal- and remainder-component kNDVIs against overall kNDVI. From left to right: trend, seasonal and remainder.

Figure 7 shows the contributions of the three STL components to the overall kNDVI dynamics. I used the R-squared values of pixel-wise linear regressions between the relevant STL component and the overall kNDVI data.

The seasonal component (that is, the annually repeating component of kNDVI) is the dominant one, with a median R-squared of 0.80 (Figure 8). However, the remainder component also plays a significant role. It has a median R-squared value of 0.152, and has a particularly high relative contribution in the north-east, portions of the Himalayas in the north, and the southernmost parts of the Western Ghats in Kerala—to name a few. The trend component has the least importance to the overall kNDVI dynamics, with a median R-squared value of 0.071.

Question 2: Sensitivity of Vegetation to Climate

Sensitivity of kNDVI components to different climate variables

Complete model:

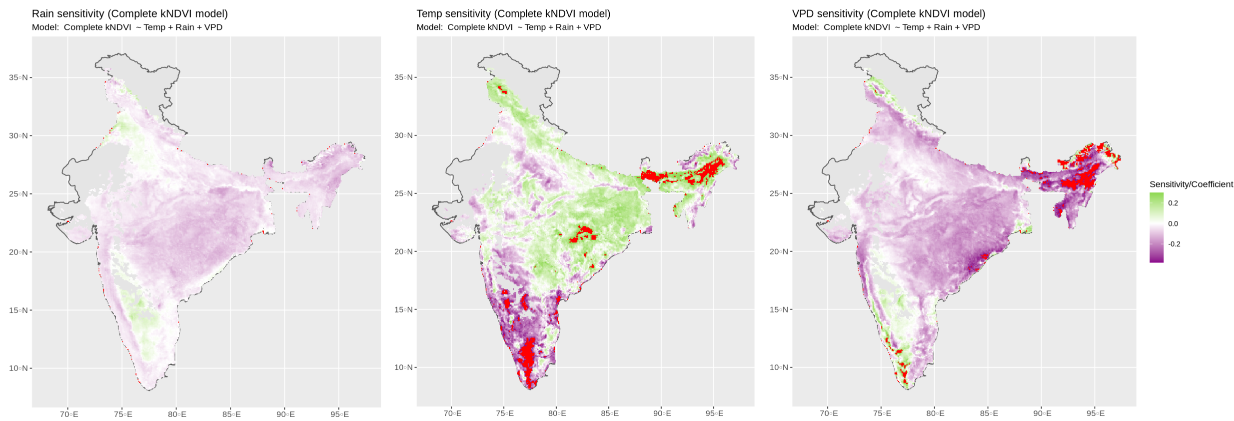

Figure 9: From left to right- maps of sensitivity of the complete kNDVI to (normalised, monthly) rain, mean temperature, and vapour pressure deficit. Sensitivity to a climate variable here is the coefficient value of the corresponding variable, from the fitted linear model kNDVI ~ Rain+Temp+VPD. The range of the plot has been limited for better visibility, and the red regions correspond to pixels with out-of-bounds values.

There are clear spatial patterns in the sensitivity of complete kNDVI to the three climatic variables. For most of the country, vegetation responds negatively to an increase in rain (all other variables held equal). Positive responses to rainfall are seen in the peninsular interior, and parts of North India. The sensitivity to rain is, in general, smaller in magnitude than the sensitivities to the other two variables.

Sensitivity to VPD shows a very similar spatial distribution to rain sensitivity. It too shows broadly negative sensitivity with positive sensitivity in the peninsular interior, but it differs from rain sensitivity in a few regions, such as Punjab.

The vegetation response to mean temperature is mostly negative in the south, and is broadly positive in the north, north-east and east India. The spatial pattern of sensitivity of complete kNDVI data to temperature is, visually, somewhat inverted with respect to the patterns of rain and VPD sensitivity.

Seasonal model

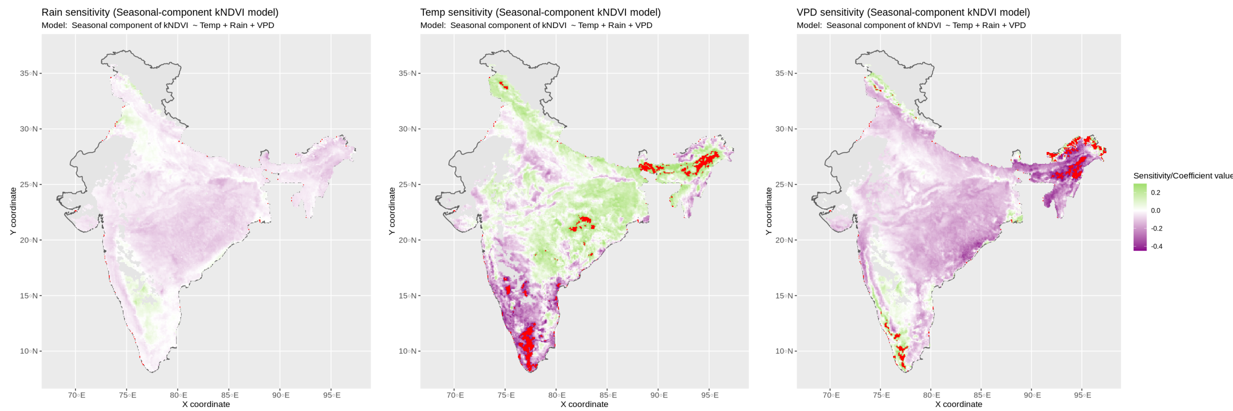

Figure 10: From left to right: maps of sensitivity of the seasonal component of kNDVI to (normalised, monthly) rain, mean temperature, and vapour pressure deficit. Sensitivity to a climate variable here is the fitted coefficient value of the corresponding variable, from the linear model Seasonal_kNDVI ~ Rain+Temp+VPD. The range of the plots have been limited for better visibility, and red corresponds to pixels with out-of-bounds values.

The spatial patterns of sensitivity of seasonal-component kNDVI to climate are very similar to the patterns of overall kNDVI sensitivity, for all three climatic variables. All the patterns noted for the complete kNDVI model hold true for the seasonal model as well.

Trend model

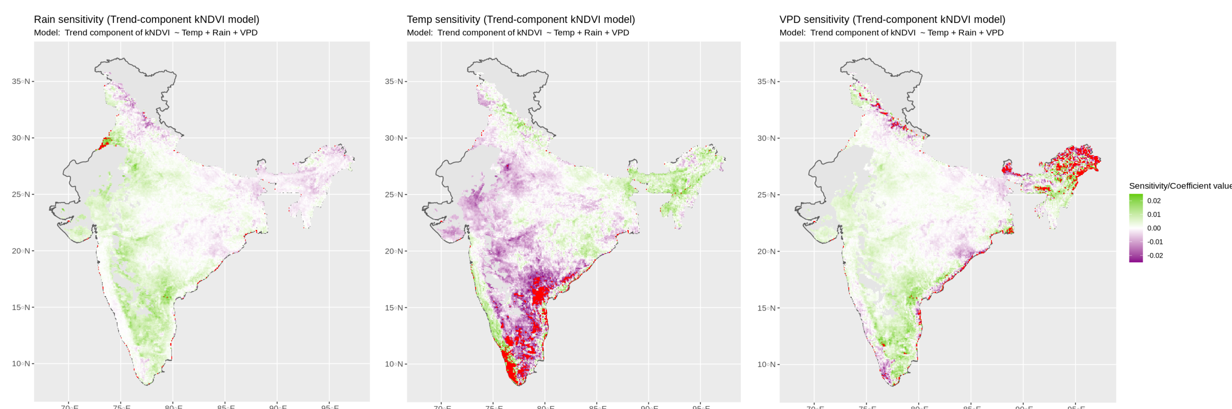

Figure 11: From left to right- maps of sensitivity of the trend component of kNDVI to (normalised, monthly) rain, mean temperature, and vapour pressure deficit. Sensitivity to a climate variable here is the fitted coefficient value of the corresponding variable, from the linear model Trend_kNDVI ~ Rain+Temp+VPD. The range of the plots have been limited for better visibility, and red corresponds to out-of-bounds values.

The rain sensitivity of the kNDVI trend component is positive over most of the country, most strongly in the north-west and in the southern peninsula. Negative sensitivity to rain is seen in the east, north-east, and in the Himalayas.

The map of trend-component VPD-sensitivity is very similar to that of rain sensitivity, but with differences in the southern Western Ghats (which shows a negative sensitivity to VPD rather than the positive/neutral sensitivity to rain) and the north-east (which shows a mosaic of positive and negative sensitivity to VPD, rather than the broadly negative response to rain).

The pattern of temperature sensitivity of the kNDVI trend component is broadly inverse in sign to the patterns of rain and VPD sensitivity. Temperature sensitivity is strongly negative in eastern peninsular India, and in north-western regions. The north-east and the Western Ghats region (both of which are dominated by forests) show positive temperature responses.

Remainder model

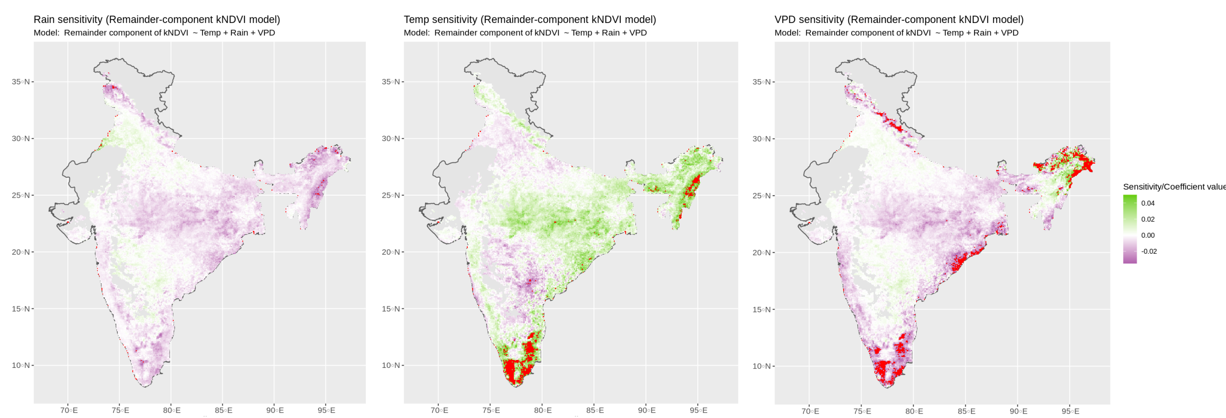

Figure 12: From left to right- maps of sensitivity of the remainder component of kNDVI to (normalised, monthly) rain, mean temperature, and vapour pressure deficit. Sensitivity to a climate variable here is the fitted coefficient value of the corresponding variable, from the linear model Remainder_kNDVI ~ Rain+Temp+VPD. The range of the plots have been limited for better visibility, and red corresponds to pixels with out-of-bounds values.

The sensitivity of the remainder-component of vegetation to rain is broadly negative. Some regions with strongly negative rain sensitivity are the north-eastern states, the northern Himalayas and a few locations in the south. There are areas of positive sensitivity to rain in the central peninsular region, and around Punjab.

Sensitivity to VPD follows a similar pattern as rain sensitivity, with the exception of areas in North-East India, which have positive coefficient values (as opposed to negative rain-sensitivity values in the same area).

The pattern of sensitivity of remainder-kNDVI to temperature is inverse to that of rain sensitivity—where rain sensitivity shows strongly positive values, temperature exhibits negative values and vice versa. The north-east, eastern, central Indian and southern areas show strong positive sensitivity to temperature.

The coefficient values for the trend-component and remainder-component of kNDVI are, in general, much smaller in magnitude than those of the seasonal component and overall kNDVI. Changes in climate have only a small effect on these components. The positive correlation between rain and VPD sensitivities is present across all the models, as is the inverse relationship between temperature sensitivity and rain/VPD sensitivity. However, it is also noticeable that in the remainder and trend models, the correlation between VPD and rain sensitivities does not hold in the north-east region.

Pixel-wise Strongest Sensitivity Variable

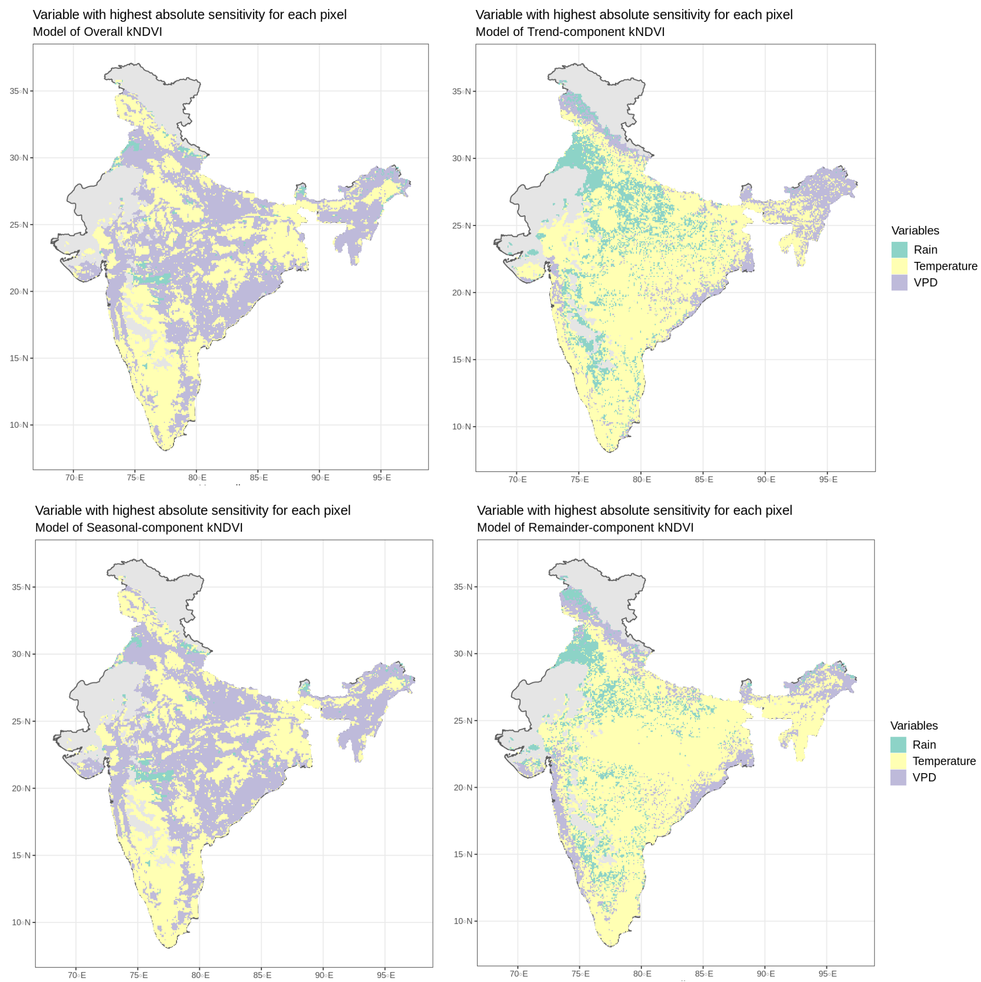

Figure 13: Maps of the climate variable which leads to the strongest vegetation response in response to a unit change in the variable. That is, the variable which, within each model, has the regression coefficient with the largest absolute value (or, the highest absolute sensitivity). From left to right- models of overall kNDVI, and the trend, seasonal and remainder components of kNDVI, as functions of rain, mean temperature and VPD.

Figure 13 maps, for every model, the variable to which vegetation has the highest absolute sensitivity. That is, it maps the variable to which vegetation responds most strongly—either in the negative or positive direction.

It is clear that the spatial distributions of variables in the seasonal-component and overall kNDVI maps are very similar to each other. This is a consequence of the fact that the seasonal component is the major contributor to the overall kNDVI data, and thus their responses are very similar both quantitatively and qualitatively.

The spatial distributions of the variables in the trend-component and remainder- component maps are also broadly similar. From figures 11 and 12, we can see that the spatial patterns of their sensitivities don't match up neatly. However, they follow similar patterns at the coarser level of which variable is the vegetation most sensitive to. This may indicate that vegetation responds to climate in a similar manner at both the trend and remainder timescales.

The seasonal-component and overall-kNDVI maps are dominated by VPD and temperature as the most important variables. On the other hand, the remainder and trend component maps are strongly dominated by temperature as the most important variable, with some patches of rain or VPD as the most important.

Correlations between sensitivities

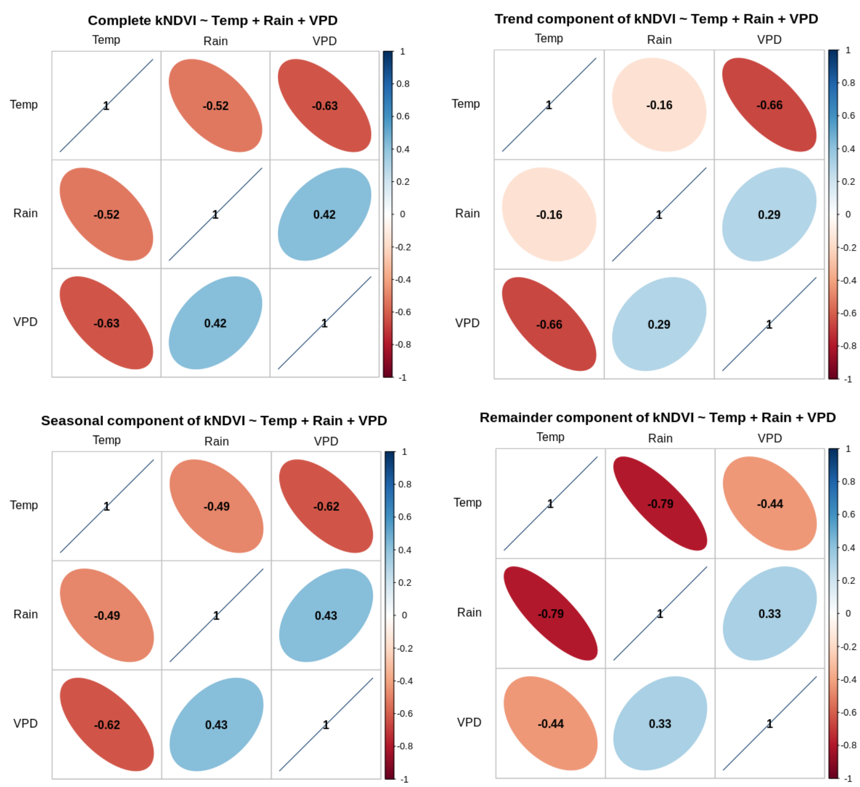

Figure 14: Correlation matrix plots of sensitivities to different climate variables, separated by kNDVI time-scale. From left to right- sensitivities of complete kNDVI, trend component, seasonal component and remainder component of kNDVI.

There is a common pattern of correlations between the climate sensitivities, across all four models:

1. Temperature and rain sensitivities are negatively correlated
2. Temperature and VPD sensitivities are negatively correlated
3. VPD and rain sensitivities are positively correlated

This quantitatively corroborates the pattern observed from the maps and noted in previous sections.

One reason for this general pattern may be the correlations between the climate variables themselves. As seen from Figure 3, the correlations between climate variables are of opposite sign to the correlation coefficients between the sensitivities to those variables—rain and VPD are negatively correlated, while rain and temperature, and temperature and VPD, are positively correlated. These correlations propagate and determine the relationships between their regression coefficients.

If two variables are positively correlated, and both are included as explanatory variables in a multiple linear regression model, then their regression coefficients will be negatively correlated. This is because if one variable is assigned a higher regression coefficient, the other will get a smaller one, because one of the two gets more 'credit' for the variance explained by the correlated component they share. Similarly if two variables are negatively correlated and are included as explanatory variables in the same model, then their regression coefficients will be positively correlated.

However, beyond the commonalities in the signs of the correlation coefficients, their magnitudes differ across models. In the remainder-component model, the Rain ~ Temp correlation is much more strongly negative than VPD ~ Temp. In the trend-component model, it is the opposite, and the magnitude of the VPD ~ Temp correlation is more than that of Rain ~ Temp. The VPD ~ Rain sensitivity relation is positive and has roughly the same magnitude in both remainder-component and trend-component models. The correlation coefficients of the seasonal and complete kNDVI models are very close in value. This continues the trend of these two models being very similar.

Since the climate variables are common to all four models, the differences must be due to the influence of other factors, and not simply an artefact of the original correlations between climate variables.

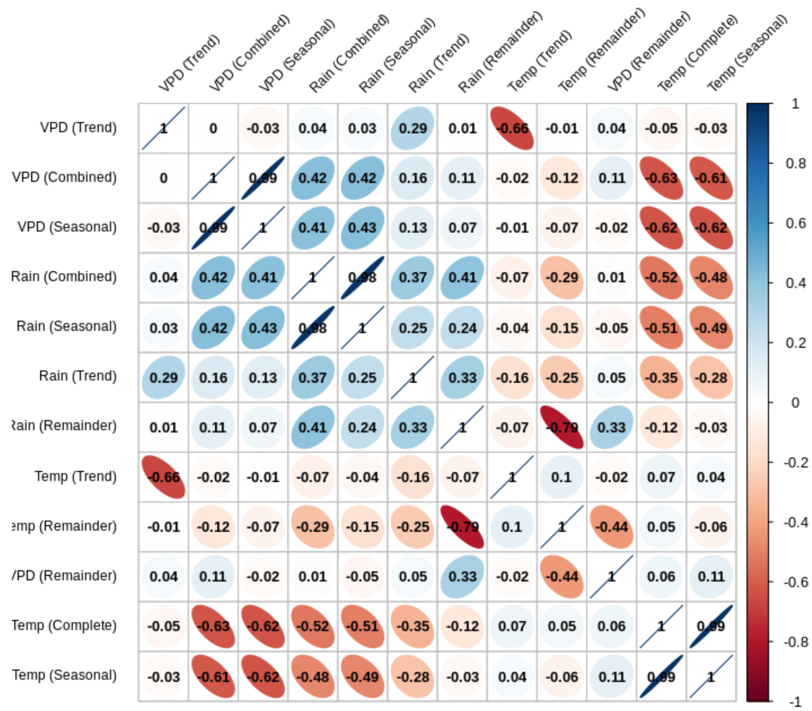

Figure 15: Matrix of the correlations between the climate sensitivities of kNDVI—that of complete kNDVI and its three time-scale components to all climate variables, across all time-scale models.

Figure 15 includes the same information as figure 14, but also plots the correlations between the sensitivities of different models. It shows quantitatively that there are very strong positive correlations (~0.99) between the sensitivities of seasonal-component and complete kNDVI to corresponding climate variables.

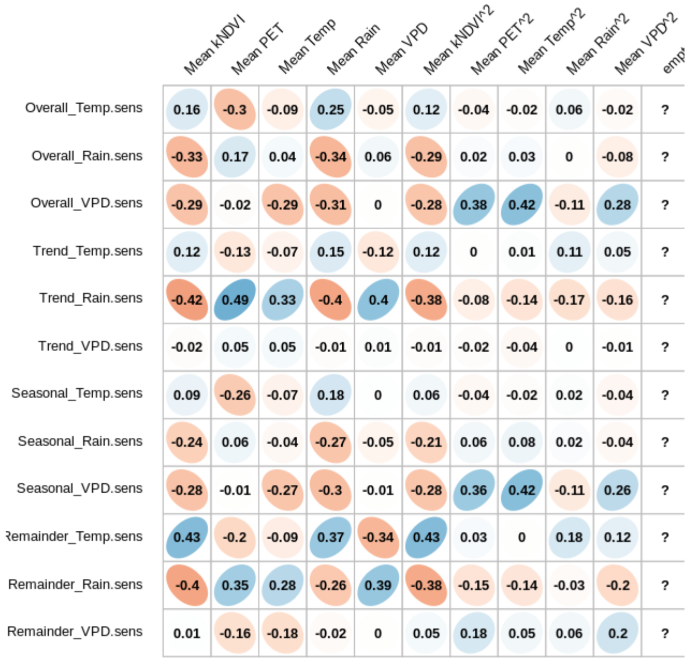

Figure 16: Plot of correlations of sensitivities (of different kNDVI components to all normalised climate variables) against mean/ background climate. Sensitivities are along the vertical axis, and background climate variables (averaged from 1982 to 2013) are along the horizontal axis.

In order to examine whether and how vegetation sensitivity is affected by background environmental variables, I calculated the correlation coefficients of sensitivities (of kNDVI components to all climate variables) against mean climate variables averaged over all time points, to find any significant linear relationships between them. I also correlated the sensitivities against the squares of mean climate variables, as a preliminary way to look for any quadratic relationships between average long-term climate and sensitivity.

From Figure 16, it is clear that there are no clear strong relationships between sensitivities and long-term average/ background climate.

Density plots were plotted to examine the same correlations between sensitivities and background climate/ squared background climate. No clear relationships, either linear or nonlinear, could be discerned from them.

Density plots correlating sensitivities to background climate were also plotted for each of the vegetation types. However, these too did not show any clear relationships between mean long-term climate and sensitivity.

Question 3: Variations due to vegetation characteristics/ land-cover classes

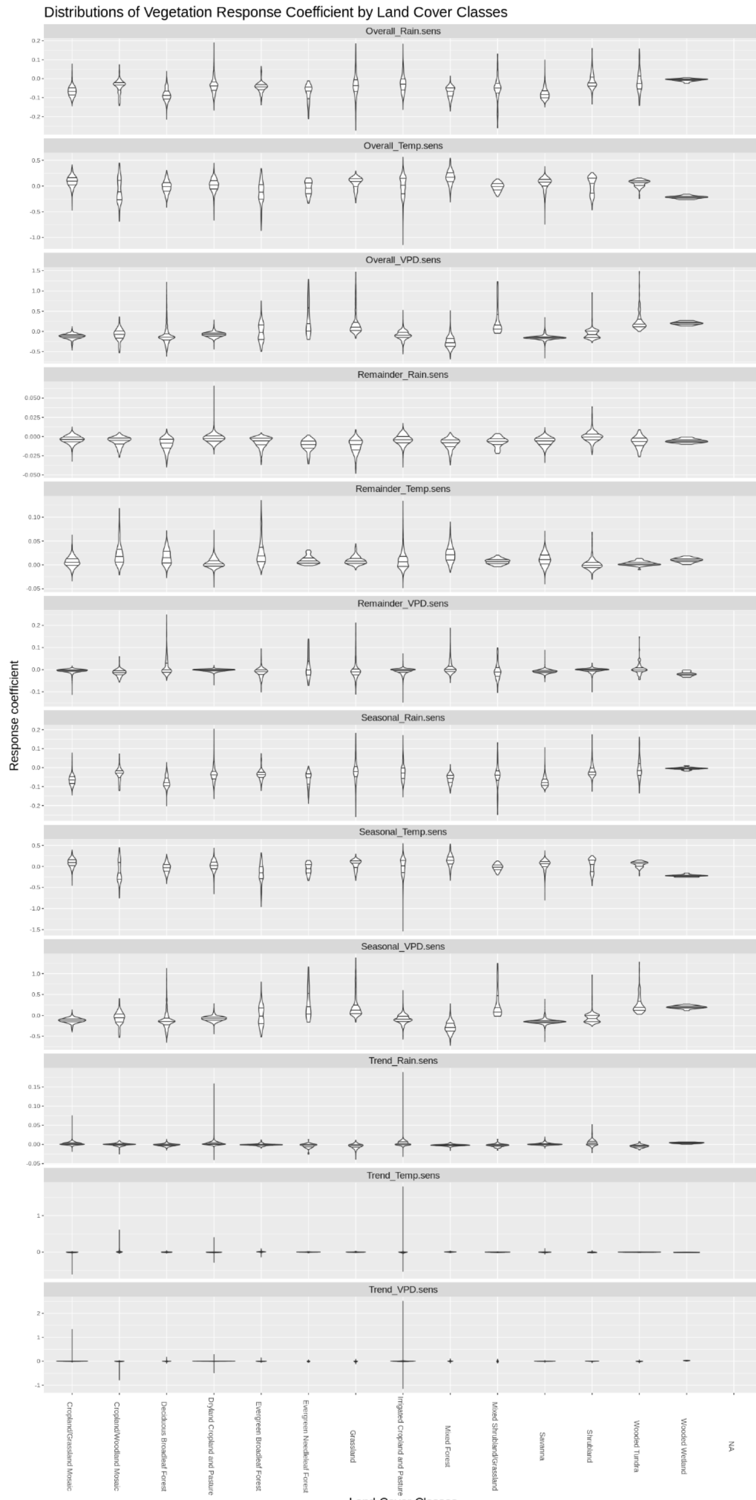

Figure 17: Violin plots showing the distributions of climate sensitivities, separated by land-cover classes (along the x-axis) and model type +climate variable (facets of the plot). The violin plots have lines indicating the median, 1st quartile and 3rd quartile. From top to bottom, the sensitivities are: Overall kNDVI sensitivity to rain, temperature, and VPD; Remainder component's sensitivity to rain, temperature, and VPD; Seasonal component's sensitivity to rain, temperature, and VPD; Trend component's sensitivity to rain, temperature and VPD. From left to right, the land-cover classes are- Cropland/grassland mosaic, Cropland/woodland mosaic, Deciduous broadleaf forest, Dryland cropland and pasture, Evergreen broadleaf forest, Evergreen needleleaf forest, Grassland, Irrigated cropland and pasture, Mixed forest, Mixed shrubland/grassland, Savanna, Shrubland, Wooded tundra, and Wooded wetland.

The sensitivity distributions for all kNDVI components and climate variables were split by land-cover type. From figure 17, there do not seem to be significant differences between land-cover classes, for most climate sensitivities. The sensitivities of the trend and the remainder components to climate are very similar across different land-cover classes. The sensitivities of the seasonal component and overall kNDVI seem to vary a bit more noticeably between land-cover classes, but even this variation is small and has no clear pattern.

In the trend component's sensitivity, the range of sensitivities to rain, temperature and VPD is very narrow for most vegetation types. However, the cropland land classes (irrigated and dry cropland+pasture, cropland/woodland mosaic, and cropland/grassland mosaic) show a wider range of sensitivities to climate. This may be due to irrigation and other human interventions (harvesting, fertilisation, etc). These interventions release the vegetation from limiting factors such as precipitation and the amount of nutrients in the soil.

Discussion

I derived many important insights from this analysis. Of the three STL components of vegetation, the seasonal timescale component is the dominant contributor to the overall kNDVI time series, with the remainder component coming in a distant second. The climate sensitivities of the seasonal and complete kNDVI are highly correlated. This is due to the very fact that the overall kNDVI data is primarily driven by the seasonal component.

Climate and other environmental variables often influence vegetation in a lagged manner. (Wu *et al.*, 2015; Liu *et al.*, 2018; Kong *et al.*, 2020) studied lags and memory effects and found that vegetation is strongly influenced by lagged climate, particularly precipitation. Including lagged climate variables improves vegetation models. While time-lags were not included in this study, they're an important consideration to include in future analyses.

The correlations between sensitivities to the different climate variables, (of complete kNDVI, and trend, seasonal, remainder components), all have the same direction/sign, and similar magnitudes of correlation coefficients. The pattern is:

- Rain sensitivity ~ Temperature sensitivity correlation is negative
- Rain sensitivity ~ VPD sensitivity correlation is positive
- Temperature sensitivity ~ VPD sensitivity correlation is negative

These are opposite in sign to the correlations between the climate variables themselves. The correlations between sensitivities make sense as an artefact of the correlations between the three climate variables (explanatory variables) themselves. When two explanatory variables are correlated positively, their regression coefficients may be negatively correlated due to a kind of 'sharing of credit' where one variable has a higher regression coefficient and the other must have a lower coefficient. This may partly explain the common pattern of correlations between sensitivities. However, the differences in this pattern between different kNDVI component models also indicate other factors at play. In the future, it would be valuable to use a method like PCR (principal components regression) or other techniques as in (Dubey and Ghosh, 2023) to disentangle the correlated climate variables.

Upon subsetting the sensitivities (of the kNDVI components to the different climate variables) by their land-cover type and comparing their distributions, I observed that there were no significant differences in median sensitivity between different vegetation types, for any of the sensitivities. This may indicate that all vegetation types in India respond to climate broadly in the same way. However, prior work (Li *et al.*, 2002; Chuai *et al.*, 2013; Wu *et al.*, 2015; Xu *et al.*, 2016; Sarvia *et al.*, 2021) shows that vegetation type is an important variable affecting responses to climate. It may be that the land-cover classification data, which was prepared from 1992-93 AVHRR satellite images, is inaccurate or outdated for other years, due to the rapid rates of land-use change. In future work, isolating and studying pixels whose land-cover type has remained unchanged may provide better data. It could also be useful to use more recent land-cover maps. It would also be important to statistically examine the differences in sensitivity distributions between vegetation types—for example, the significance of sensitivity differences between vegetation types. Another explanation may be that the calculation of a single sensitivity value from 30 years of data flattened the differences between vegetation types—with any differences being very small in magnitude. Examining changes in sensitivity over time by carrying out linear regressions on a sliding window, or shifting regression (Piao *et al.*, 2014; Myers-Smith *et al.*, 2015; Ratzmann *et al.*, 2016) may be worthwhile for future work.

On correlating sensitivities to the background climate of each pixel (calculated by averaging climate variables over all time points), no clear patterns or relationships could be found. This was true both for the complete dataset and subsets of it by vegetation type. In further work, it may be more helpful to study sensitivity as a function of background climate using better methods than simple linear regression (like non-linear regression, machine learning techniques, etc.), as linear regression may be missing the meaningful relationships between sensitivity and climate. It may also be worthwhile to model sensitivity as a function of other non-climate environmental variables.

References

Abatzoglou, JT, Dobrowski, SZ, Parks, SA, and Hegewisch, KC (2018). TerraClimate, a high-resolution global dataset of monthly climate and climatic water balance from 1958–2015. Sci Data 5, 170191.

Abel, C, Horion, S, Tagesson, T, De Keersmaecker, W, Seddon, AWR, Abdi, AM, and Fensholt, R (2021). The human–environment nexus and vegetation–rainfall sensitivity in tropical drylands. Nat Sustain 4, 25–32.

Alkama, R, Forzieri, G, Duveiller, G, Grassi, G, Liang, S, and Cescatti, A (2022). Vegetation-based climate mitigation in a warmer and greener World. Nat Commun 13, 606.

Bao, Z, Zhang, J, Wang, G, Guan, T, Jin, J, Liu, Y, Li, M, and Ma, T (2021). The sensitivity of vegetation cover to climate change in multiple climatic zones using machine learning algorithms. Ecological Indicators 124, 107443.

Camps-Valls, G et al. (2021). A unified vegetation index for quantifying the terrestrial biosphere. Science Advances 7, eabc7447.

Canadell, JG et al. (2021). Global Carbon and Other Biogeochemical Cycles and Feedbacks. In: Climate Change 2021: The Physical Science Basis. Contribution of Working Group I to the Sixth Assessment Report of the Intergovernmental Panel on Climate Change, ed.Intergovernmental Panel on Climate Change (IPCC), Cambridge: Cambridge University Press, 673–816.

Chuai, XW, Huang, XJ, Wang, WJ, and Bao, G (2013). NDVI, temperature and precipitation changes and their relationships with different vegetation types during 1998–2007 in Inner Mongolia, China. International Journal of Climatology 33, 1696–1706.

Cleveland, R, Cleveland, WS, McRae, JE, and Terpenning, IJ (1990). STL: A seasonal-trend decomposition procedure based on loess (with discussion).

Deng, S, Yang, T, Zeng, B, Zhu, X, and Xu, H (2013). Vegetation cover variation in the Qilian Mountains and its response to climate change in 2000–2011. J Mt Sci 10, 1050–1062.

Diao, C, Liu, Y, Zhao, L, Zhuo, G, and Zhang, Y (2021). Regional-scale vegetation-climate interactions on the Qinghai-Tibet Plateau. Ecological Informatics 65, 101413.

Ding, Y, Li, Z, and Peng, S (2020). Global analysis of time-lag and -accumulation effects of climate on vegetation growth. International Journal of Applied Earth Observation and Geoinformation 92, 102179.

Dubey, N, and Ghosh, S (2023). The relative role of soil moisture and vapor pressure deficit in affecting the Indian vegetation productivity. Environ Res Lett 18, 064012.

Farquhar, GD (1997). Carbon Dioxide and Vegetation. Science 278, 1411–1411.

Funk, CC, Peterson, PJ, Landsfeld, MF, Pedreros, DH, Verdin, JP, Rowland, JD, Romero, BE, Husak, GJ, Michaelsen, JC, and Verdin, AP (2014). A quasi-global precipitation time series for drought monitoring, Reston, VA: U.S. Geological Survey.

Green, JK, Konings, AG, Alemohammad, SH, Berry, J, Entekhabi, D, Kolassa, J, Lee, J-E, and Gentine, P (2017). Regionally strong feedbacks between the atmosphere and terrestrial biosphere. Nature Geosci 10, 410–414.

Guhathakurta, P, and Rajeevan, M (2008). Trends in the rainfall pattern over India. International Journal of Climatology 28, 1453–1469.

Gulev, SK et al. (2021). Changing State of the Climate System. In: Climate Change 2021: The Physical Science Basis. Contribution of Working Group I to the Sixth Assessment Report of the Intergovernmental Panel on Climate Change, ed. V Masson-Delmotte et al., Cambridge, United Kingdom and New York, NY, USA: Cambridge University Press, 287–422.

He, Y, Guo, X, Dixon, P, and Wilmshurst, JF (2012). NDVI variation and its relation to climate in Canadian ecozones. Canadian Geographies / Géographies Canadiennes 56, 492–507.

India Meteorological Department. (last) (2017). “Frequently Asked Questions (FAQ)” (PDF). Wayback Machine. Available at: https://web.archive.org/web/20170310143225/http://imd.gov.in/section/nhac/wxfaq.pdf. Accessed January 1, 2024.

Kim, JH (2019). Multicollinearity and misleading statistical results. Korean J Anesthesiol 72, 558–569.

Kong, D, Miao, C, Wu, J, Zheng, H, and Wu, S (2020). Time lag of vegetation growth on the Loess Plateau in response to climate factors: Estimation, distribution, and influence. Science of The Total Environment 744, 140726.

Kusch, E, Davy, R, and Seddon, AWR (2022). Vegetation-memory effects and their association with vegetation resilience in global drylands. Journal of Ecology 110, 1561–1574.

Li, B, Tao, S, and Dawson, RW (2002). Relations between AVHRR NDVI and ecoclimatic parameters in China. International Journal of Remote Sensing 23, 989–999.

Li, J, Bevacqua, E, Chen, C, Wang, Z, Chen, X, Myneni, RB, Wu, X, Xu, C-Y, Zhang, Z, and Zscheischler, J (2022). Regional asymmetry in the response of global vegetation growth to springtime compound climate events. Commun Earth Environ 3, 1–9.

Liu, L, Zhang, Y, Wu, S, Li, S, and Qin, D (2018). Water memory effects and their impacts on global vegetation productivity and resilience. Sci Rep 8, 2962.

Myers-Smith, IH et al. (2015). Climate sensitivity of shrub growth across the tundra biome. Nature Clim Change 5, 887–891.

Nie, Q, Xu, J, Ji, M, Cao, L, Yang, Y, and Hong, Y (2012). The Vegetation Coverage Dynamic Coupling with Climatic Factors in Northeast China Transect. Environmental Management 50, 405–417.

P., S, and Paul, S (2021). Spatio-temporal dependency of vegetation dynamics on climatic variables during 1982–2015 over India. Advances in Space Research 68, 4616–4635.

Parida, BR, Pandey, AC, and Patel, NR (2020). Greening and Browning Trends of Vegetation in India and Their Responses to Climatic and Non-Climatic Drivers. Climate 8, 92.

Peel, MC, Finlayson, BL, and McMahon, TA (2007). Updated world map of the Köppen-Geiger climate classification. Hydrology and Earth System Sciences 11, 1633–1644.

Pettorelli, N, Vik, JO, Mysterud, A, Gaillard, J-M, Tucker, CJ, and Stenseth, NC (2005). Using the satellite-derived NDVI to assess ecological responses to environmental change. Trends in Ecology & Evolution 20, 503–510.

Piao, S et al. (2014). Evidence for a weakening relationship between interannual temperature variability and northern vegetation activity. Nat Commun 5, 5018.

Piao, S, Mohammat, A, Fang, J, Cai, Q, and Feng, J (2006). NDVI-based increase in growth of temperate grasslands and its responses to climate changes in China. Global Environmental Change 16, 340–348.

Ratzmann, G, Gangkofner, U, Tietjen, B, and Fensholt, R (2016). Dryland Vegetation Functional Response to Altered Rainfall Amounts and Variability Derived from Satellite Time Series Data. Remote Sensing 8, 1026.

Sarvia, F, De Petris, S, and Borgogno-Mondino, E (2021). Exploring Climate Change Effects on Vegetation Phenology by MOD13Q1 Data: The Piemonte Region Case Study in the Period 2001–2019. Agronomy 11, 555.

Seddon, AWR, Macias-Fauria, M, Long, PR, Benz, D, and Willis, KJ (2016). Sensitivity of global terrestrial ecosystems to climate variability. Nature 531, 229–232.

Sedjo, R, and Sohngen, B (2012). Carbon Sequestration in Forests and Soils. Annual Review of Resource Economics 4, 127–144.

Terrer, C et al. (2021). A trade-off between plant and soil carbon storage under elevated CO2.

Nature 591, 599–603.

Wang, F, Wang, X, Zhao, Y, and Yang, Z (2014). Temporal variations of NDVI and correlations between NDVI and hydro-climatological variables at Lake Baiyangdian, China. Int J Biometeorol 58, 1531–1543.

Wang, J, Rich, PM, and Price, KP (2003). Temporal responses of NDVI to precipitation and temperature in the central Great Plains, USA. International Journal of Remote Sensing 24, 2345–2364.

Wang, S, and Fan, F (2021). Analysis of the Response of Long-Term Vegetation Dynamics to Climate Variability Using the Pruned Exact Linear Time (PELT) Method and Disturbance Lag Model (DLM) Based on Remote Sensing Data: A Case Study in Guangdong Province (China). Remote Sensing 13, 1873.

Wu, D, Zhao, X, Liang, S, Zhou, T, Huang, K, Tang, B, and Zhao, W (2015). Time-lag effects of global vegetation responses to climate change. Global Change Biology 21, 3520–3531.

Xu, Y, Yang, J, and Chen, Y (2016). NDVI-based vegetation responses to climate change in an arid area of China. Theor Appl Climatol 126, 213–222.

Zhang, Y et al. (2022). Increasing sensitivity of dryland vegetation greenness to precipitation due to rising atmospheric CO_2. Nat Commun 13, 4875.

(2023). Asia. In: Climate Change 2022 – Impacts, Adaptation and Vulnerability: Working Group II Contribution to the Sixth Assessment Report of the Intergovernmental Panel on Climate Change, ed.Intergovernmental Panel on Climate Change (IPCC), Cambridge: Cambridge University Press, 1457–1580.